Journal of Chemical, Biological and Physical Sciences

An International Peer Review E-3 Journal of Sciences

*Available online at*www.jcbsc.org

Section A: Chemical Sciences

CODEN (USA): JCBPAT Research Article

Performance and Theoretical Study of Corrosion Inhibition of Mild Steel in 2M Hydrochloric Acid Solution by N-Benzyl Piperidin-4-one Semicarbazones

K. Raja [1], A.N. Senthilkumar [2], S. Umamatheswari [1] and K. Tharini [1*]

[1] Post Graduate & Research Department of Chemistry, Government Arts College, Trichirappalli, India

[2] Post Graduate & Research Department of Chemistry, Alagappa Government Arts College, Karaikudi, India.

Received: 28 October 2016**; Revised:** 12 November 2016**; Accepted:** 30 November 2016

Abstract: Acid solutions are used in industries during various processes such as acidic cleaning, pickling and oil well acidification which generally leads to serious metallic corrosion. It has been found that one of the best methods of protecting metals against corrosion involves the use of inhibitors. Inhibitors are added to the acid solution to minimize acid attack on metal. A large number of organic compounds including heterocyclic compounds were studied as corrosion inhibitors for mild steel. Most of inhibitors are toxic and expensive so the research activities in recent times are geared towards developing cheap, non-toxic and environmentally safe corrosion inhibitors. The present paper describes a study of N-benzyl piperdin-4-one thiosemicarbazone (BPTSC) and N-benzyl piperdin-4-one semicarbazone (BPSC) as corrosion inhibitors for mild steel in 2M hydrochloric acid using potentiodynamic weight loss, polarization, impedance measurements, SEM with EDS and quantum chemical studies.

Keywords: BPTSC, BPSC, weight loss, polarization, impedance, SEM with EDS and quantum chemical studies.

INTRODUCTION

Corrosion inhibitors are generally used in industries to minimize both the metal loss and acid consumption [1] many organic compounds have been analyzed for their utility as corrosion inhibitors in acid media [2]. These molecules act at the inter phase (created by corrosion product) between the metal and aqueous corroding solution [3]. Nature of inhibitor interaction and efficiency may be dependent on the chemical, mechanical and structural characteristic of this layer. Organic compounds that serve as effective inhibitors must have at least one functional group or heteroatom and/or aromatic ring to act as primary center for adsorption process [4, 5]. However ,choice of an inhibitor for a particular system is a difficult task due to its selectivity and specificity. Synthesis of new organic molecules with diverse molecular structures containing several heteroatom and substituents satisfy the above needs. The influence of two newly synthesized nitrogen containing semicarbazone, namely, N-benzyl piperdin-4-one thiosemicarbazone (BPTSC) and N-benzyl piperdin-4-one semicarbazone (BPSC) on the corrosion of mild steel in 2M HCl by weight loss method, polarization, impedance measurements and SEM with EDS and quantum chemical calculation have been studied here.

EXPERIMRNTAL

Procedure for preparation of N-benzyl piperidin -4-one semicarbazone: To the boiling solution of N-benzyl piperidin -4-one (0.01mol) in methanol (45ml) and few drops of concentrated hydrochloric acid, the methanolic solution of semicarbazide hydrochloride (0.01 mol) was added drop wise by stirring. The reaction was refluxed for 4 hours on a water bath. After cooling, the solid product was filtered and recrystallized from methanol to get the corresponding semicarbazone.

Procedure for preparation of N-benzyl piperidin -4-one thiosemicarbazone: To the boiling solution of N-benzyl piperidin -4-one (0.01mol) in methanol (45ml) and few drops of concentrated hydrochloric acid, the methanolic solution of thiosemicarbazide hydrochloride (0.01 mol) was added drop wise by strirring. The reaction was refluxed for 4 hours on a water bath. After cooling, the solid product was filtered and recrystallized from methanol to get the corresponding thiosemicarbazone.

Table-1: Characterization of N-benzyl piperidin-4-one derivatives.

Compound Name	Yield (%)	Melting point(^{0}C)	Elemental analysis
N-benzyl piperidin-4-one semicarbazone	92	165-167	C(%) 63.43 H(%)7.29 N(%) 22.65
N-benzyl piperidin-4-one thio semicarbazone	95	158-160	C(%) 59.69 H(%)7.09 N(%) 21.28

Weight loss method: Mild steel coupons of composition (%) Mn=0.272, Si=0.190, S=0.028, P=0.017, Cr=0.021, Mo=0.006, Ni: 0.012, C=0.039 and Fe=99.415 were used. They were cut into specific dimensions of 4x1x0.2 cm and grounded with different grades of emery papers, washed thoroughly with doubled distilled water, degreased and dried using acetone. The aggressive solution of 2M HCl was prepared using double distilled water. The coupons were immersed in presence and absence of various concentrations of BPTSC and BPSC in 2 M HCl for 1hr and 2hrs time intervals at temperatures 303K, 313K, 323K and 333K. From the loss of weight of these coupons, the percentage inhibition efficiency (IE) and corrosion rate (CR) were calculated.

Polarization and impedance measurements: Electrochemical studies were carried out with CH electrochemical analyzer Model No: 604 C at room temperature by using mild steel specimens of 1 cm^2 area as working electrode. The saturated calomel electrode and platinum electrodes were used as reference and counter electrodes, respectively. AC impedance measurements were carried out at E_{corr} values after immersion on standing in air atmosphere. Tafel plots and Nyquist plots were recorded by the usual procedure [6-8]. IE values were calculated from the I_{corr} values.

SEM with EDS: The nature of the film formed on the surface of the metal specimens was analyzed by energy dispersive X-ray analysis (EDS) using JOEL instrument in conjugation with an energy dispersive spectrometer. The spectra were recorded on samples immersed in the presence and absence of inhibitor in corrosive medium for a period of 2h.

RESLUTS AND DISCUSSION

Spectral analysis: BPSC: yield:92%; IR (cm-1) 3409,3252 (N-H stretching); 1684 (C=O stretching); 1620 (C=N stretching); 1H NMR (δ ppm) : 4.38 (t, 2H, H-2); 3.15 (t, 2H, H-6); 2.73 (t, 2H, H-3); 1.98 (t, 2H, H-5); 4.30 (s, 2H, -N-CH2-Ph); 4.29 (s,1H, NH proton)7.48-7.65 (m, 10H, aryl protons); 13C NMR (δ ppm): 51.58 (C-2); 49.20 (C-6); 30.08 (C-3); 23.54 (C-5); 152.77 (C=N); 159.01 (C=O); 60.21 (-N-CH_2-Ph); 131.33- 128.29 (aromatic carbons).

BPTSC: Yield:95% ; IR (cm-1) 3387 (N-H stretching), 1599 (C=N stretching); 3206 (NH_2 stretching); 1H NMR (δ ppm) : 4.51 (t, 2H, H-2); 3.15 (t, 2H, H-6); 2.71 (t, 2H, H-3); 1.90 (t, 2H, H-5); 3.98 (s, 2H, -N-CH2-Ph); 8.1 (s, 1H, NH proton); 10.34 (s, 2H, NH proton)7.47-7.43 (m, 10H, aryl protons). 13C NMR (δ ppm): 51.48 (C-2); 50.37 (C-6); 31.70 (C-3); 25.21 (C-5); 168.22 (C=N); 178.84 (C=S); 59.30 (-N-CH_2-Ph); 140.44, 130.36 and 128.58 (aromatic carbons).

Weight loss studies: From the weight loss values, the IE and surface coverage of each concentration were calculated using the following equations:

$$\% IE = \theta \times 100 = [(Wo - W)/ Wo] \times 100 \quad \ldots (1)$$

$$= \theta = 1- (Wo - W) \quad \ldots (2)$$

Where Wo and W are the values of the average weight losses without and with addition of the inhibitor, respectively.

Table-1 shows the values of IE and CR obtained from weight loss measurements for different concentrations of BPTSC and BPSC at four temperature viz. 303K, 313K, 323K and 333K in 1hr and 2hrs duration. As evident from **Table-1**, IE of all of these compounds increases with increase in inhibitor concentration. The maximum IE for each compound was achieved at 300ppm and further increases in concentration did not cause any appreciable change in the performance of the inhibitors.

The order of IE is BPTSC>BPSC. Inhibition of corrosion of mild steel in HCl by BPTSC and BPSC can be explained on the basis of molecular adsorption. In acid solution, inhibitors can act as cathodic as well as anodic species. The BPTSC and BPSC molecule can be protonated in acid solution forming a cation [9]. The cationic species may adsorb on the cathodic sites of the mild steel and reduce the evolution of hydrogen and thereby protecting the cathodic sites of mild steel.

Table-2: Calculated values of corrosion rate and inhibition efficiency for mild steel in 2 M HCl in the absence and presence of BPTSC at 303K-333K in one hour duration.

	Concentration	303K		313K		323K		333K	
		IE	CR	IE	CR	IE	CR	IE	CR
BPSC (1hr)	25	77.09	0.15	71.37	0.16	61.14	0.26	55.89	0.31
	50	80.21	0.13	72.16	0.16	63.32	0.24	57.65	0.3
	100	83.34	0.11	74.09	0.15	66.33	0.22	60.4	0.28
	200	88.03	0.08	76.93	0.13	68.81	0.21	61.57	0.27
	300	89.8	0.06	78.35	0.12	69.33	0.2	62.26	0.26
BPSC (2hrs)	25	81.07	0.08	73.53	0.12	65.24	0.29	56.62	0.33
	50	85.38	0.06	75.45	0.11	70.07	0.25	58.15	0.32
	100	87.5	0.05	77.5	0.1	71.55	0.24	61.29	0.29
	200	88.87	0.05	79.4	0.09	72.19	0.23	62.89	0.28
	300	90.91	0.04	81.62	0.08	73.34	0.22	63.42	0.28
BPTSC (1hr)	25	84.62	0.14	79.93	0.2	74.4	0.23	68.66	0.31
	50	87.72	0.11S	82.02	0.18	75.23	0.23	69.42	0.3
	100	89.67	0.09	83.23	0.17	77.25	0.21	70.47	0.29
	200	90.75	0.08	84.44	0.16	79.63	0.19	71.3	0.28
	300	92.41	0.07	84.84	0.15	81.08	0.17	72.07	0.27
BPTSC (2hrs)	25	86.89	0.15	80.47	0.26	79.93	0.29	75.41	0.33
	50	87.95	0.13	81.37	0.25	80.5	0.28	75.61	0.33
	100	89.56	0.11	81.75	0.24	80.79	0.28	76.17	0.32
	200	90.36	0.1	83.22	0.22	81.79	0.27	76.57	0.32
	300	91.42	0.09	84.27	0.21	81.19	0.26	77.15	0.31

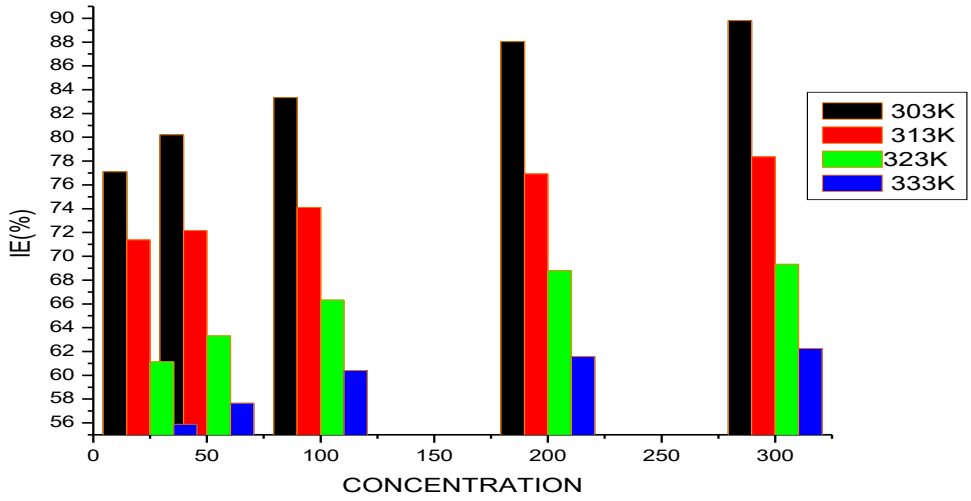

Figure 1: Plot of inhibition efficiency Vs concentration of (BPSC) at 1 hour duration.

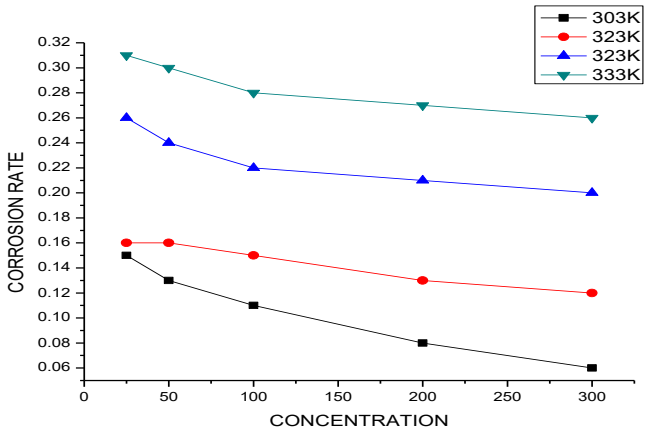

Figure 2: Plot of corrosion rate Vs concentration of (BPSC) at 1 hour duration.

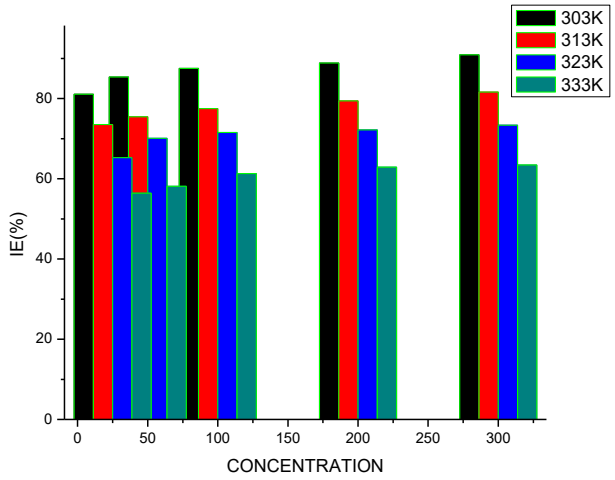

Figure 3: Plot of inhibition efficiency Vs concentration of (BPSC) at 2 hours duration.

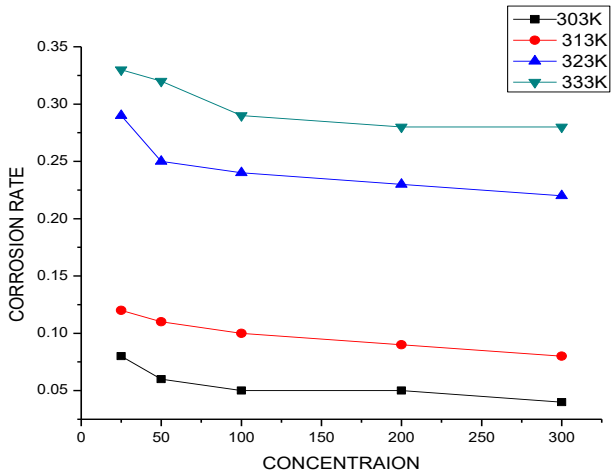

Figure 4: Plot of corrosion rate Vs concentration of (BPSC) at 2 hours duration.

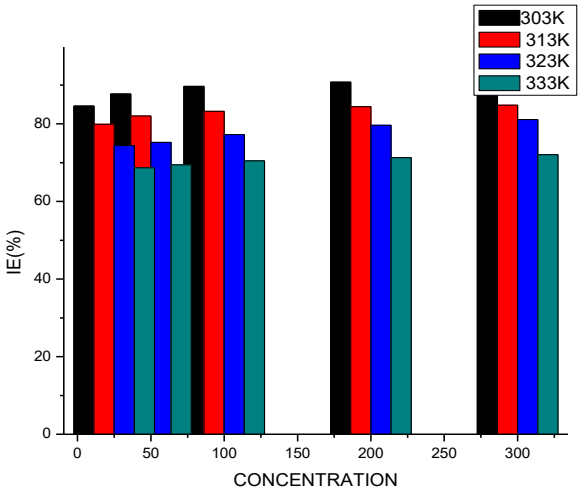

Figure 5: Plot of inhibition efficiency Vs concentration (BPTSC) at 1 hour duration.

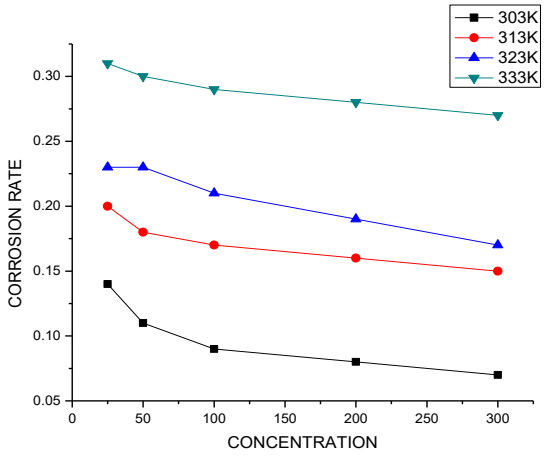

Figure 6: Plot of corrosion rate Vs concentration of (BPTSC) at 1 hour duration

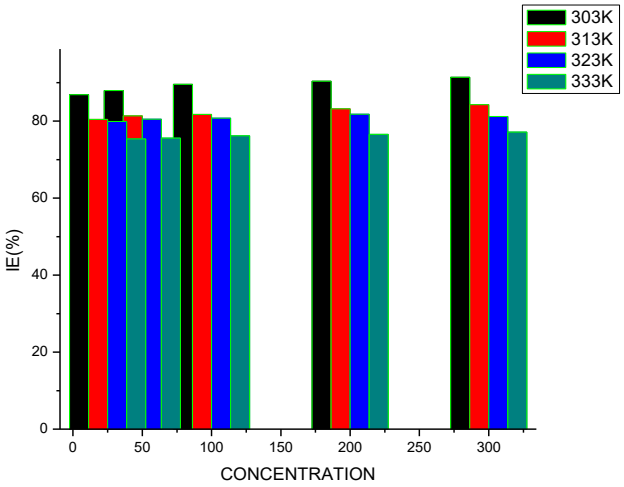

Figure 7: Plot of inhibition efficiency Vs concentration of (BPTSC) at 2 hours duration.

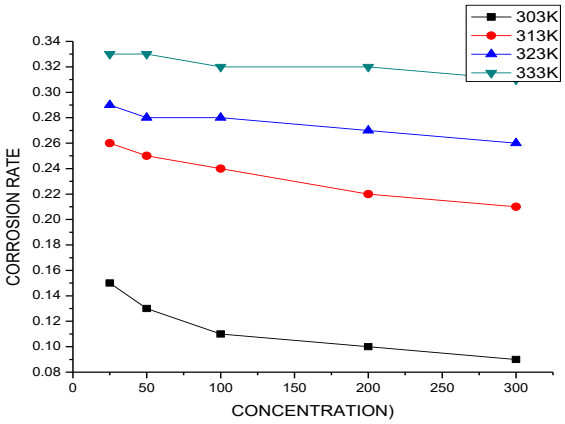

Figure 8: Plot of corrosion rate Vs concentration of (BPTSC) at 2 hour duration.

The adsorption of inhibitor at anodic sites can be attributed to the presence of lone pair of electron N and Π electronic clouds of phenyl rings which favor adsorption of these compounds on the metal surface. It has been observed that the IE of the BPTSC and BPSC decreases with an increase in temperature from 303K to 333K, due to the desorption of the inhibitor molecules from the metal surface. The values of activation energy (E_a) were calculated using the Arrhenius equation. It is found that the E_a values of the inhibited systems are higher than those of the uninhibited systems, which indicate that inhibitors are effective at the temperature of 303K and IE decreases with an increase in temperature [10]. In order to understand the mechanism of corrosion inhibitor, the adsorption behavior of the organic adsorbate on the metal surface must be known [11]. θ for different concentration of inhibitors in HCl have been evaluated from weight loss values as given in Eq.(2).

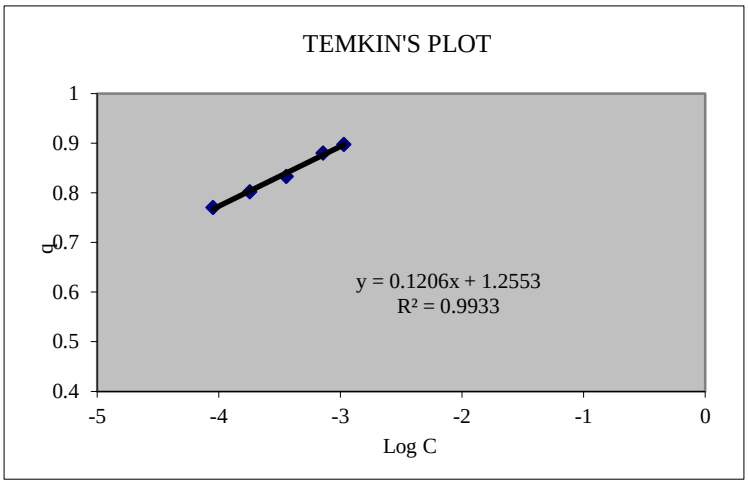

Figure 9: Temkin's plot for mild steel specimen exposed in 2M HCl medium in presence of BPTSC at 303K.

The data were tested graphically by fitting it to various isotherm. A straight line was obtained on plotting θ Vs log C (representative graph is shown in **Figure 9**) and to suggesting that the adsorption of the compounds in HCl on the mild steel surface follows Temkin's adsorption isotherm.

The free energy of adsorption ΔG_{ads} was calculated using slopes and intercepts of above isotherm, which reveals the physical mode of adsorption. The negative values of free energy of adsorption (BPTSC: -36291.0 and BPSC: -51918.2) indicate spontaneous adsorption of the inhibitors on the surface of mild steel [12].

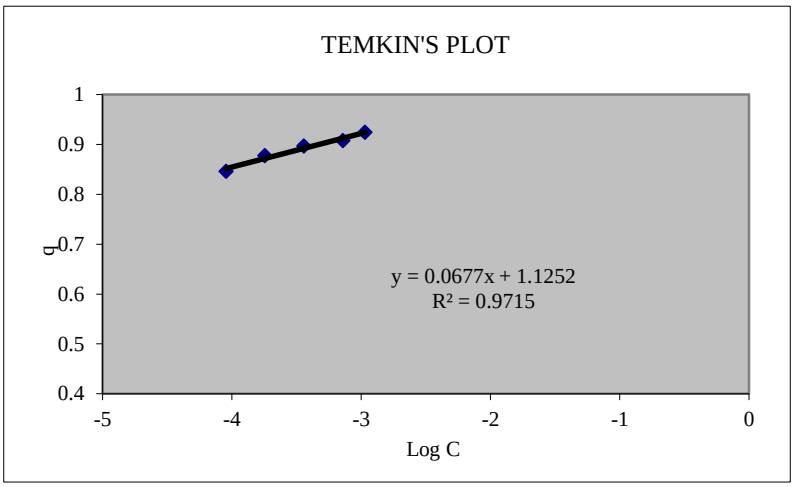

Figure 10: Temkin's plot for mild steel specimen exposed in 2M HCl medium in presence of BPSC at 303K.

Polarization measurements: Table-3 shows the data for potentiodynamic polarization curves and Nyquist plot for the mild steel in 2M HCl in presence and absence of inhibitor. As evident from the data, corrosion current (i_{corr}) values decrease with increase of inhibitor concentration thereby suppressing corrosion process. Corrosion potential (E_{corr}) values were not shifted in any particular direction. The rationale for the above observation could be attributed to the blocking of cathodic sites by physisorption and simultaneous hindering of anodic oxidation process by electron rich sites present in piperidine moiety, which control corrosion [13]. The Tafel constants b_a and b_c values did not show deviation in any particular direction with increase of inhibitor concentration. This suggests that mechanism involves simple blocking of reaction site [14] involving mixed mode mechanism. The i_{corr} values show that BPTSC offers maximum hindrance to corrosion current and behaves as excellent inhibitor among the two. The results correlated well with weight loss measurements.

Impedance study: The interpretation of Nyquist plot data from **Table-3** helps to determine the charge transfer resistance (R_{ct}) and double layer capacitance (C_{dl}). The Nyquist plots were not perfect semicircles because of dispersing effect [15]. **Table-3** clearly indicates that R_{ct} values increase while C_{dl} values decrease with increase of BPTSC and BPSC concentration resulting in the increase of IE. The decrease of C_{dl} values is due to the adsorption of inhibitor on mild steel surface. Adsorption can occur either by donor – acceptor interaction between the π electrons /nonbonded electrons of inhibitor and the vacant d orbitals of Fe atoms present in mild steel or interaction of BPTSC /BPSC with already absorbed chloride ions from HCl [16, 17]. Adsorption is also negatively charged mild steel surface. Among the two inhibitors , BPTSC shows maximum efficiency as evident from **Table-3** .This may be due to the +I effect offered by the two nitrogen groups, which increase the availability of lone pair of electrons cloud of the two phenyl rings. The ring nitrogen can also be expected to donate its electrons for coordination.

Table-3: Tafel plot of electrochemical parameters of BPTSC and BPSC in 2M HCl medium.

Compound	Concentration of inhibitor (ppm)	$-E_{corr}$ mV	I_{corr} μAcm^{-2}	$-b_a$ mV dec^{-1}	$-b_c$ mV dec^{-1}	C_{dl} $\mu F\ cm^{-2}$	R_{ct} $\Omega\ cm^2$	% of IE
BPSC	Blank	480	434	58	26	218	21	---
	25	478	292	60	28	179	110	80.9
	50	482	215	43	32	144	119	82.3
	100	502	201	75	34	112	146	85.6
	200	485	179	68	66	85	156	86.5
	300	506	152	64	85	54	188	88.8
BPTSC	Blank	0.4798	0.211	80	107	103.9	11.06	-
	25	0.462	0.1632	51	95	98.3	61.16	81.88
	50	0.4735	0.181	105	108	96.8	82.17	86.62
	100	0.4931	0.53	43	54	88.2	98.81	88.79
	200	0.4682	0.0765	72	67	82.6	103.51	89.31
	300	0.4696	0.0691	35	58	67.8	168.14	93.58

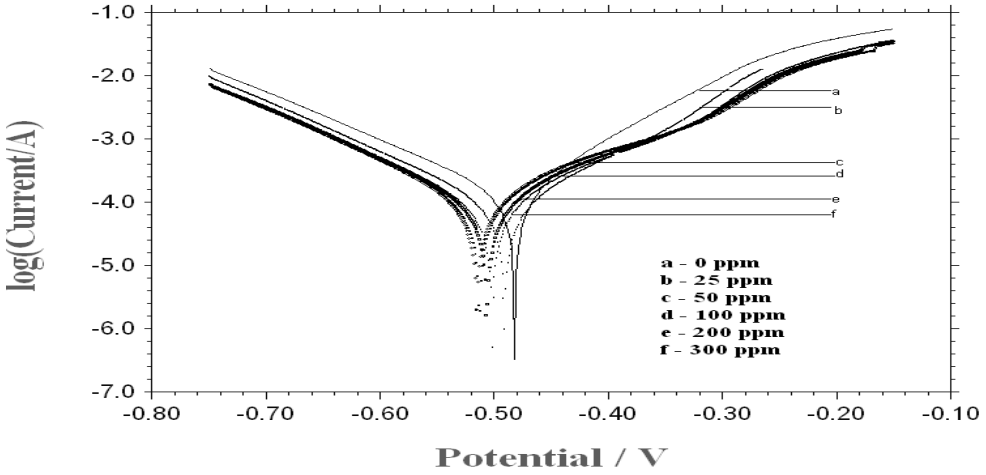

Figure 11: Tafel lines for mild steel corrosion in 2 M hydrochloric acid in the presence of various concentration of BPSC inhibitor.

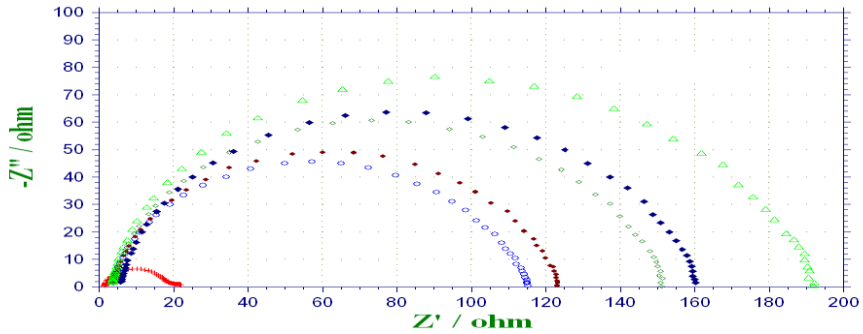

Figure 12: Nyquist plots for mild steel corrosion in 2M hydrochloric acid in the absence and the presence of various concentration of BPSC inhibitor.

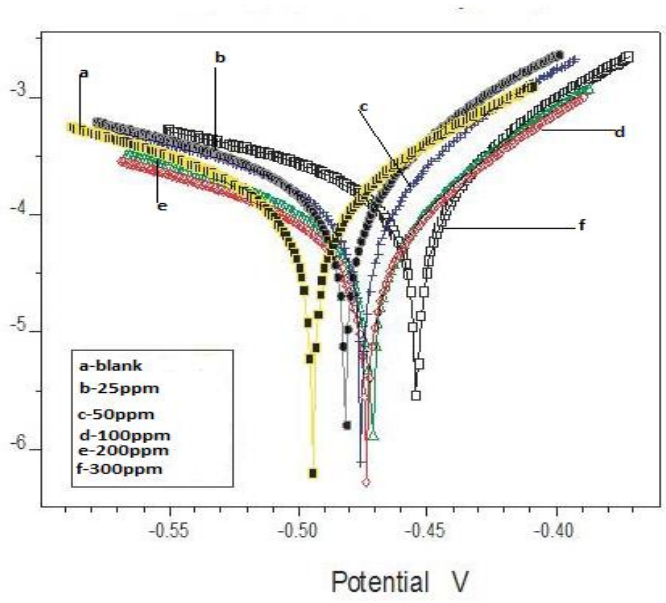

Figure 13: Different concentration and inhibition efficiency in BPTSC at two hours duration.

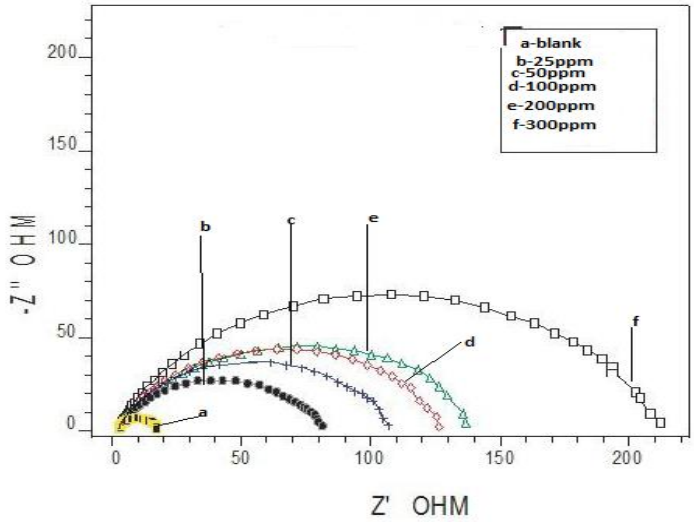

Figure 14: Nyquist plots for mild steel corrosion in 2 M hydrochloric acid in the absence and the presence of various concentration of BPTSC inhibitor at two hours duration.

SEM with EDS analysis: SEM analysis for the mild steel immersed in 2M HCl with and without BPTSC and BPSC is shown in **Figure 15** to **17**. Careful comparison of the figure reveals the formation of protective film over mild steel by BPTSC and BPSC. EDS results show that BPTSC morphology in **Figure 16** still contains oxidized phases, but their relative abundance was less as compared with the blank. Absence of Cl and increased percentage Fe in BPTSC data provide strong evidence for the formation of protective barrier.

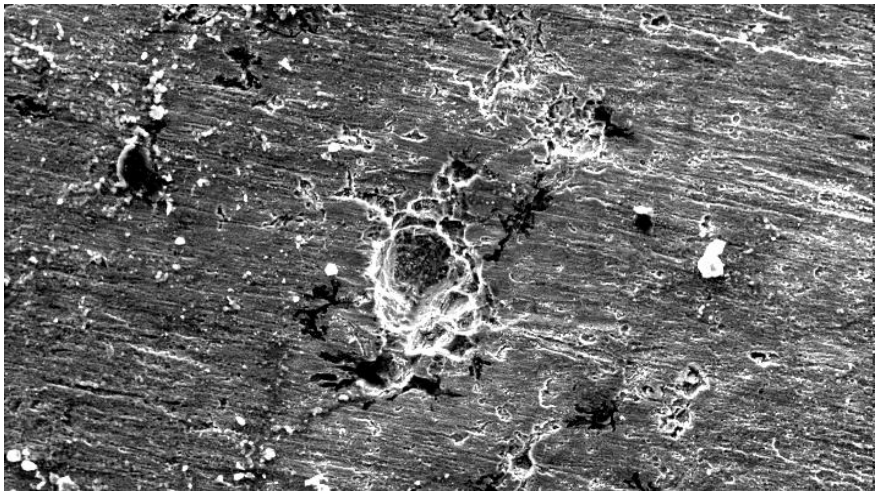

Figure 15: Micrograph of brightly polished MS surface exposed to 2M HCl.

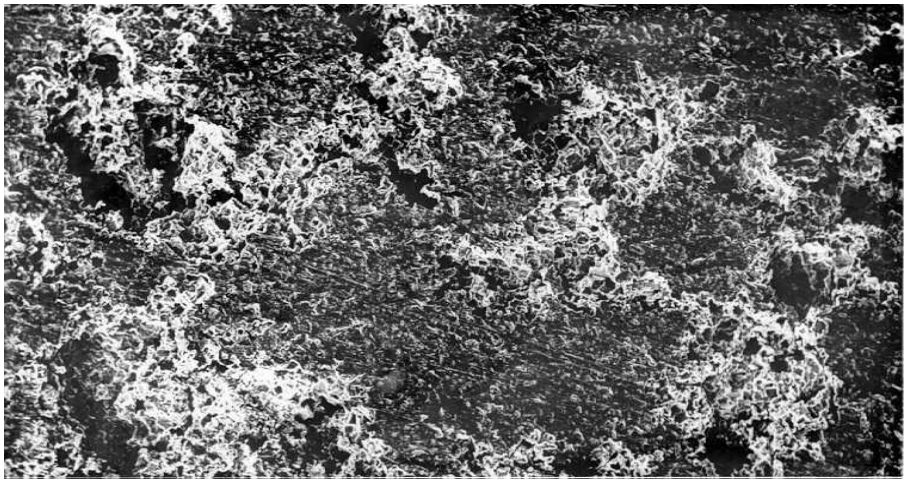

Figure 16: SEM analysis of MS surface exposed to BPTSC 2M HCl.

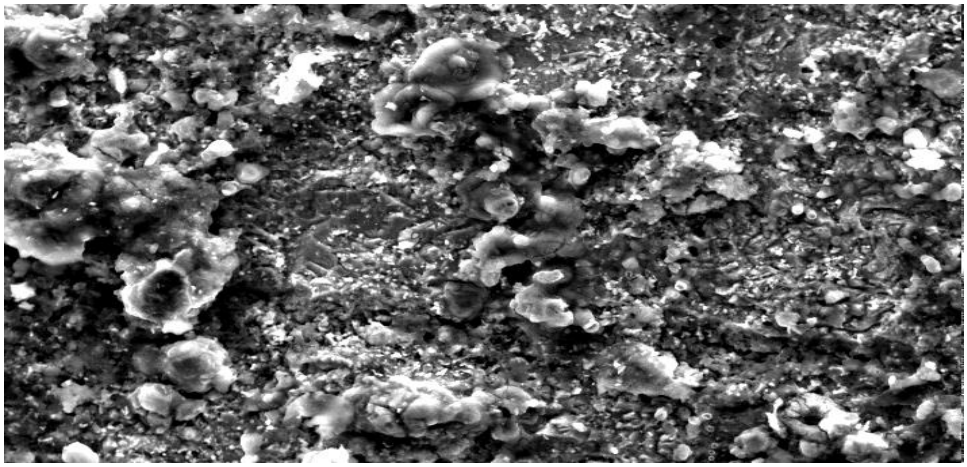

Figure 17: SEM analysis of MS surface exposed to BPSC in 2M HCl.

Quantum Chemical Calculations: All the calculations were done by means of B3LYP/6-31g (d) at DFT method [13-17]. These methods can reach exactitude similar to other methods in less time and with a smaller investment from the computational point of view. This approach is shown to yield favourable geometries for a wide variety of systems. This basis set gives good geometry optimizations.

The geometry structure was optimized under no constraint. The following quantum chemical parameters were calculated from the obtained optimized structure: The highest occupied molecular orbital (E_{HOMO}) and the lowest unoccupied molecular orbital (E_{LUMO}), the energy difference (ΔE) between E_{HOMO} and E_{LUMO}, dipole moment (μ), electronegativity (χ), electron affinity (A), global hardness (η), global softness (σ), ionization potential (I) and the fraction of electrons transferred (ΔN).

According to Koopman's theorem, the ionization potential (E) and electron affinity (A) of the inhibitor are calculated using the following equations.

$$E = -E_{HOMO} \quad \ldots (1)$$

$$A = -E_{LUMO} \quad \ldots (2)$$

Electronegativity

$$\chi = \frac{E+A}{2} \quad \ldots (3)$$

Chemical hardness

$$\eta = \frac{E-A}{2} \quad \ldots (4)$$

Global chemical softness

$$\sigma = \frac{1}{\eta} = -\frac{2}{E_{HOMO}-E_{LUMO}} \quad \ldots (5)$$

Transferred electrons

$$\Delta N = \frac{\chi_{Fe}-\chi_{inh}}{2(\eta_{Fe}+\eta_{inh})} \quad \ldots (6)$$

Where χ_{Fe} and χ_{inh} denote the absolute electronegativity of iron and inhibitor molecule, η_{Fe} and η_{inh} denote the absolute hardness of iron and the inhibitor molecule respectively. In this study, we use the theoretical value of χ_{Fe} =7.0 eV and χ_{inh} = 0, for calculating the number of electrons transferred.

The optimized molecular structure and HOMO-LUMO of the BPTSC and BPSC are shown in **Figure 18** and **19**. From **Figures 18** and **19** it can be seen that the electronic density in HOMO and LUMO on the entire area of each molecule are quite uniform which is due to its lone pair of electron of nitrogen and π-electron cloud density of phenyl ring.

The analysis of orbital HOMO and LUMO (**Figures 18** and **19**) implies that the preferential area of nucleophilic attack to the inhibitor is the 1-benzyl ring as well as nitrogen and sulfur atoms of semicarbazone and thiosemicarbazone.

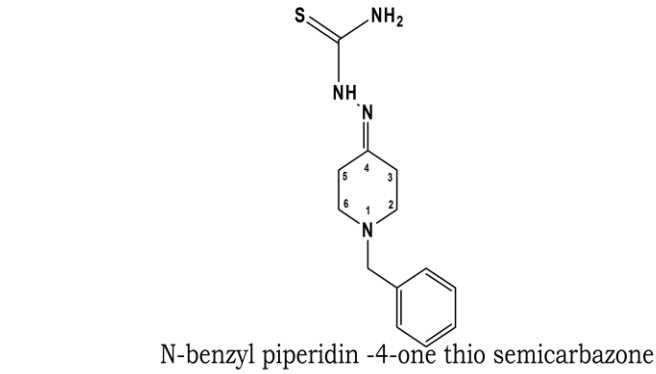

N-benzyl piperidin -4-one thio semicarbazone

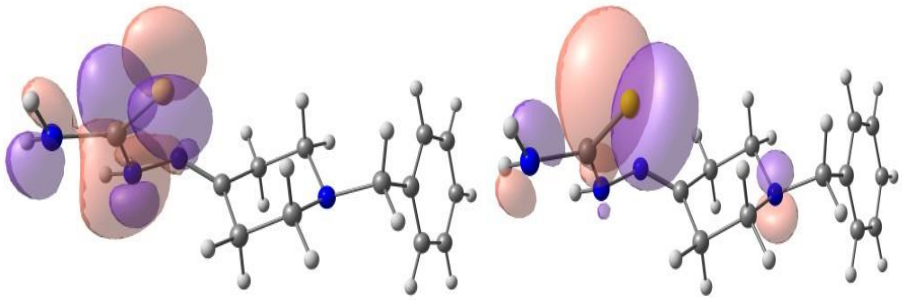

2_HOMO 2_LUMO

Figure 18: N-benzyl piperidin-4-one thiosemicarbazone.

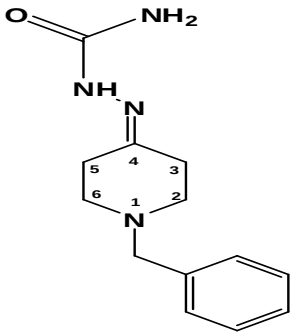

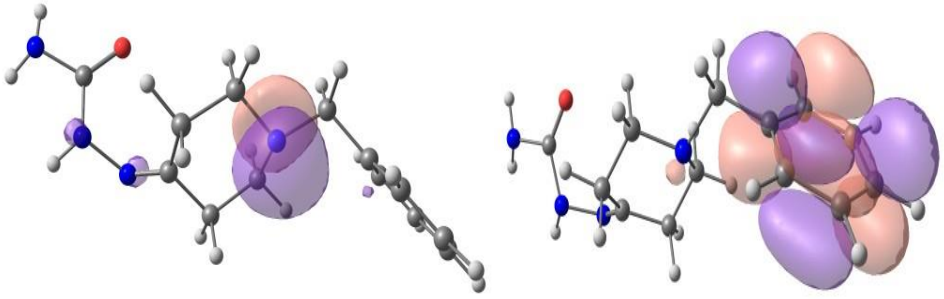

3_HOMO **3_LUMO**

Figure 19: N-benzyl piperidin-4-one semicarbazone.

Table 4: Calculated quantum chemical parameters of the studied inhibitor.

Quantum parameters	**BPSC**	**BPTSC**
E_{HOMO} (eV)	-6.1051	-5.4638
E_{LUMO} (eV)	-0.4493	-0.8270
ΔE gap (eV)	5.66	4.64
μ (debye)	4.25	6.42
I= $-E_{HOMO}$ (eV)	6.1051	5.4638
A= $-E_{LUMO}$ (eV)	0.4493	0.8270
$\chi = \frac{I + A}{2}$	3.2772	3.1454
$\eta = \frac{I - A}{2}$	2.8279	2.3184
$\sigma = \frac{1}{\eta}$	0.3536	0.4313
$\omega = \mu^2/2\eta$	3.1936	8.8897
$\Delta N = \frac{\chi_{Fe} - \chi_{inh}}{2(\eta_{Fe} + \eta_{inh})}$	0.6582	0.8313
TE(eV)	-21780.81	-30568.93

CONCLUSION

The following conclusions can be drawn from the present study. The compounds tested were proved to inhibit the mild steel from corrosion in 2M HCl . The replacement of oxygen by sulfur increased the inhibition efficiency of N-benzyl piperidin -4-one thiosemicarbazone. The studied compounds acted as mixed type inhibitors in 2M HCl . With the increases in the concentration of inhibitors, the active sites of adsorption increased, which prevented the mild steel from corrosion. The results obtained from weight loss test and electrochemical measurements were in good agreement. The inhibitors show significant corrosion inhibition activity in a dose dependent manner. The inhibitors affect both cathodic and anodic Tafel slopes in acid and act through mixed mode. SEM images offer a perfect proof for the formation of protective layer of inhibitor over mild steel surface, thus preventing corrosion. Quantum chemical studies have been successfully performed to link the corrosion inhibition efficiency with molecular orbital's (MO) energy levels for BPTSC and BPSC. Our results confirmed the strong correlation between these microscopic electronic properties and corrosion inhibition efficiencies. Substitution of the carbonyl (>C=O) of semicarbazone by the group of thiocarbamoyl (>C=S) leads to the transfer of chelation center from each pair of nitrogen atom to the sulphur atom in thiocarbamoyl of thiosemicarbazone molecules, significantly resulting in the increase of HOMO level and a great reduce of HOMO–LUMO energy difference. This gives a believable explanation for the increase of inhibition efficiency due to the substitution of (>C=O) by (>C=S). That is, thiocarbamoyl group plays predominant role in terms of forming coordinate covalent bonds and/or feedback bonds with metal surface through chemical adsorption.

REFERENCES

1. R.E. Melchers, R. Jeffery. *Corrosion Reviews*. 2005, **1**, 84.
2. R.E. Melchers, R. Jeffery. *Corrosion Reviews*. 2005, **6**, 297.
3. G. Saha, N. Kurmaih, N. Hakerman. *J. Physis. Chem*. 1955, **59**, 707.
4. M.G. Fontana. Corrosion Engineering. 3rd ed., McGraw-Hill Book Company, New York. 1987, 346.
5. M. Abdallah. *Corros. Sc*. 2002, **44**, 717.
6. S.M.A. Hossini, M. Salari. *Indian Journal of Chemical Technology*. 2009, **16,** 480.
7. S.D. Shetty, P. Shetty, H.V.S. Nayak. *J. Serb. Chem. Soc. 2006,* **71**, 1073.
8. P.K. Gogoi, B. Barhai. *Int. J. Chem*. 2010, **2**, 218.
9. K. Adardour, O. Kassou, R. Touir, M. Ebn Touhami, H. El Kafsaoui, H. Benzeid, M. Essassi, M. Sfaira. *J. Mater. Environ. Sci*. 2010, **1**, 129.
10. M.A. Quraishi, Rawat. *J., Mat. Chem. Phys*. 2002, **73,** 118.
11. H. Nazyl, H. Rudolf. *J. Chem. Sci*. 2009, **121**, 693.
12. A.N. Senthilkumar, K. Tharini, M.G. Sethuraman. *Surf Rev Lett*. 2009, **16**, 1 141.
13. A.N. Senthilkumar, K. Tharini, M.G. Sethuraman. *Acta Phy Chim Sin*. 2012, **28**, 2, 399.
14. A.N. Senthilkumar, K. Tharini, M.G. Sethuraman. *J Mat Eng & Perfo*. 2011, **26**, 2, 969.
15. A.E. Stoyanova, E.I. Sokolova, S.N. Raicheva. *Corros*. 1997, **39**, 9, 1595.
16. V. Baliah, C.R. Noller. *J. Am. Chem. Soc*. 1948, **70**, 3853.
17. A.N. Senthilkumar, M.G. Sethuraman. *Corr. Rev*. 2008, **26**, 1, 23.

***Corresponding author: K. Tharini;**

Post Graduate & Research Department of Chemistry, Government Arts College, Trichirappalli, India.